

# Structure Formation in High-Performance PBO Fibers

S. Ran<sup>1</sup>, C. Burger<sup>1</sup>, D. Fang<sup>1</sup>, D. Cookson<sup>2,3</sup>, K. Yabuki<sup>4</sup>, Y. Teramoto<sup>4</sup>,

P.M. Cunniff<sup>5</sup>, P.J. Viccaro<sup>3</sup>, B.S. Hsiao<sup>1</sup>, and B. Chu<sup>1\*</sup>

<sup>1</sup>Chemistry Department, SUNY Stony Brook, Stony Brook, NY

<sup>2</sup>Australian Nuclear Science and Technology Organization, Menai NSW, Australia

<sup>3</sup>ChemMat CARS, Advanced Photon Source, Argonne National Laboratory, Argonne, IL

<sup>4</sup>Toyobo Co. Ltd., Research Center, Katata, Ohtsu, Shiga, Japan

<sup>5</sup>U.S. Army, Soldier and Biological Chemical Command, Natick, MA

Poly-*p*-phenylenebenzobisoxazole (PBO) (Figure 1) forms the strongest synthetic polymer fiber known so far. It provides excellent mechanical properties paired with extreme thermal stability, making PBO the optimum material for applications like lightweight bulletproof vests and fire-resistant suits.

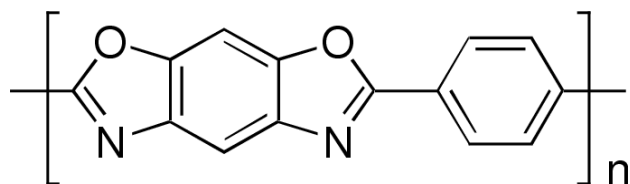


**Figure 1.** Chemical structure of poly-*p*-phenylenebenzobisoxazole (PBO).

PBO is spun from a lyotropic melt in polyphosphoric acid (PPA) under stretching by an adjustable spin-draw ratio (SDR). PPA is removed by coagulation in a water bath, resulting in the as-spun (AS) fiber, which is subsequently heat-treated to form the final high-modulus (HM) fiber. It is the goal of the present study to understand the structural evolution of the PBO fiber throughout different processing stages using synchrotron small-angle and wide-angle x-ray scattering (SAXS/WAXS) techniques.

## Experimental

A spinning apparatus consisting of a capillary rheometer-like barrel with an upper temperature capability of 300° C, a vertical precision movement to shift different fiber regions into the beam, a motor driven plunger, a take-up wheel with adjustable speed providing defined spin draw ratios, and a coagulation water bath has been set up at beamline X27C of the National Synchrotron Light Source (NSLS) at Brookhaven National Laboratory (BNL) (Figure 2). Further experimental details were given in [1]. The PBO-PPA solution (dope) has been provided by Toyobo Co. *In situ* wide-angle x-ray scattering (WAXS) and small-angle x-ray

scattering (SAXS) 2D patterns were recorded using a MAR CCD detector. Furthermore, WAXS and SAXS measurements have been performed after extended coagulation and after heat treatment in vacuum or under nitrogen.

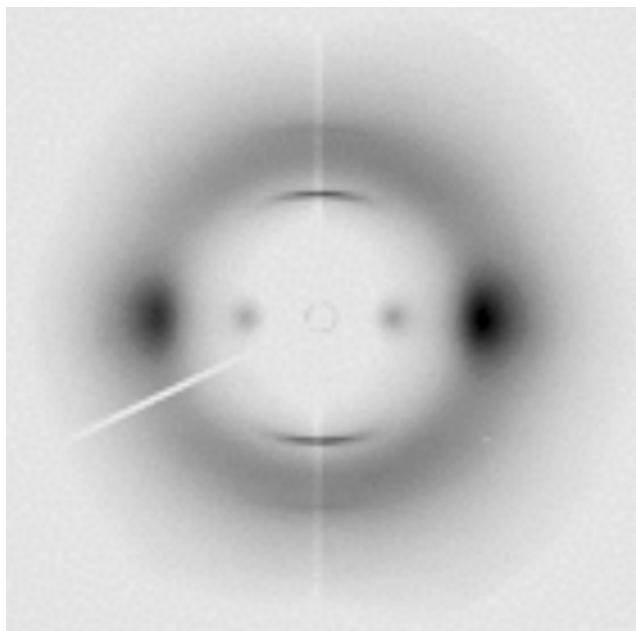
## Results and Discussion

Figures 3(a) and 3(b) show *in situ* WAXS patterns of the PBO fiber before and after passing through the coagulation water bath, respectively. The two patterns consist mainly of meridional streaks (due to the monomer period) and of equatorial arcs describing the lateral packing order and indicating a high degree of preferred orientation. The absence of off-axis reflections indicates a translational disorder in the fiber direction in either case. A close inspection of the two WAXS patterns before and after coagulation shows that the equatorial peak positions and, thus, the corresponding lateral packing spacings are different. The pattern before coagulation (Figure 3(a)) shows two equatorial maxima not following a classical position ratio (like  $1:\sqrt{3}$  for 2D hexagonal) and a weaker intensity for the lower angle



**Figure 2.** PBO *in situ* spinning apparatus with MAR CCD detector at beamline X27C in NSLS, BNL.

(a) before coagulation



(b) after coagulation

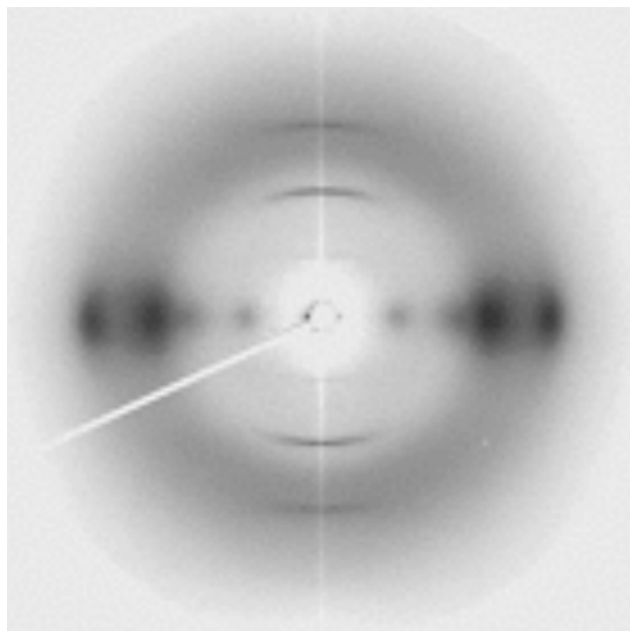


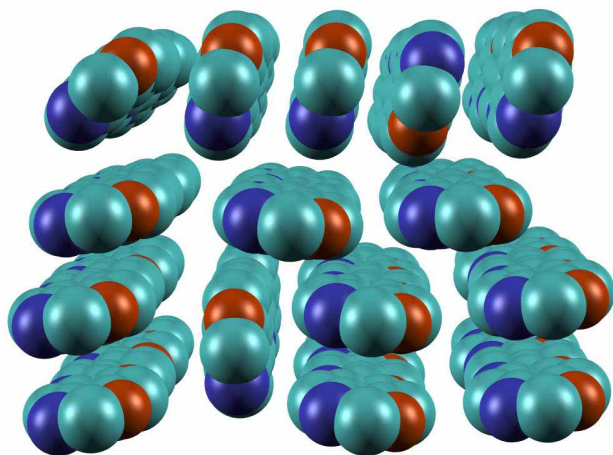
**Figure 3.** In situ WAXS patterns of the PBO fiber before and after passing through the coagulation water bath (fiber axis vertical).

peak. This can be interpreted in terms of a liquid-crystalline packing of plank-shaped structural units. The lateral packing of the anisometric cross-sections leads to two distinct spacings giving rise to the observed equatorial peaks. This situation is known as “sanidic” liquid-crystalline order. The nature of the plank-shaped structural units is not exactly known; it is believed to be a well-defined solvate complex of PBO and PPA.

For the coagulated PBO fiber, the structures interpreted from the observed WAXS data range from a

sanidic liquid-crystalline pattern with two equatorial length scales, where now the single PBO molecule is the plank-shaped structural unit (Figure 4(a)) to a higher ordered structure which, apart from the translational disorder, approaches the ideal crystalline PBO structure (Figure 4(b)). A characteristic feature of the sanidic phase, with liquid-crystalline short-range order in the cross-section, is a preferred formation of stacks (Figure 4(a)) with higher intra-stack order enhancing the equatorial peak at higher angles corresponding to the

(a) sanidic lyotropic order: formation of stacks



(b) 2D ordered cross-section; translational disorder

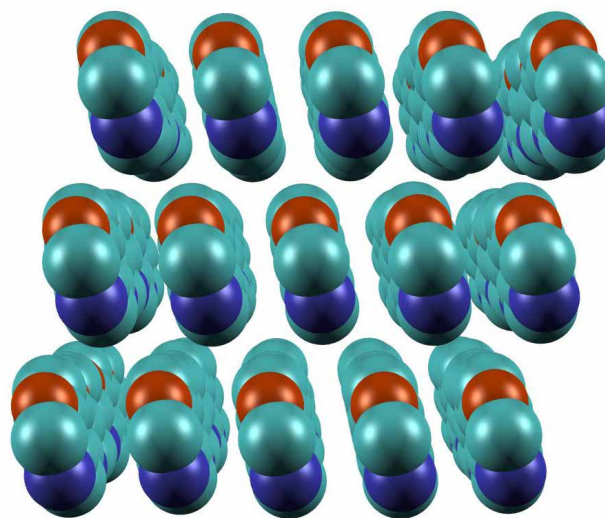


**Figure 4.** Structure models illustration different degrees of order in the packing of PBO molecules.

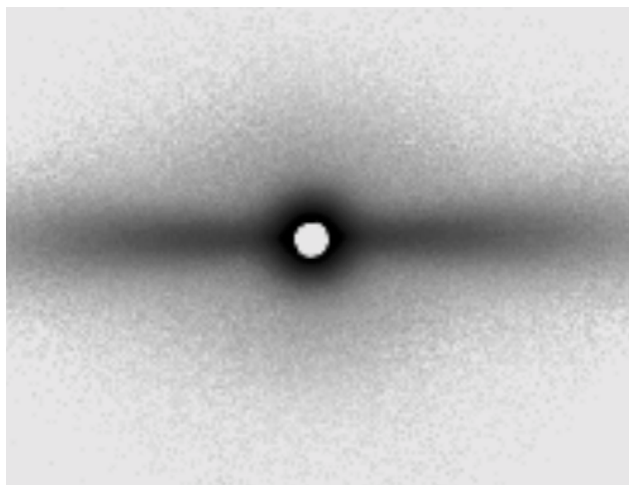
stacking period, and a less ordered lateral packing of stacks explaining the weaker intensity of the lower angle equatorial peak. The transition to the higher ordered structure, forming a true 2D lattice in the cross-section (Figure 4(b)) can be observed by the appearance of mixed  $hk0$  reflections on the equator, most notably the 2-10 for PBO.

Figure 5 shows SAXS patterns of as-spun PBO (fully coagulated but not yet heat-treated), high modulus PBO (heat-treated, this is the final form of the high-performance fiber) and PBO fibers which were subjected to an extended heat treatment (EHT), degrading the local structure and the mechanical properties. The AS fiber only shows an equatorial streak (Figure 5(a)) due to elongated microvoids and/or multiple scattering from a fibrillar structure. After heat treatment, a SAXS four-point pattern is observed (Figure 5(b)). An extended heat treatment is able to enhance this four-point pattern (Figure 5(c)). The corresponding WAXS pattern, as well as the poor mechanical properties of the EHT fiber, suggests that it underwent a chemical degradation of the structure which is apparently able to enhance the contrast of the four-point pattern. However, it was not clear so far whether this chemical reaction is the original cause of the four-point pattern or whether it only contrasts a pre-existing structure. Recent high-brilliance experiments at the ChemMAT CARS beamline at the Advance Photon Source, Argonne National Lab, involving a highly collimated, focused beam probing PBO single filaments in a full vacuum setup, were able to show the existence of the four-point pattern already in the AS fiber, proving that a chemical reaction during the heat treatment is not the original cause of the four-point pattern.

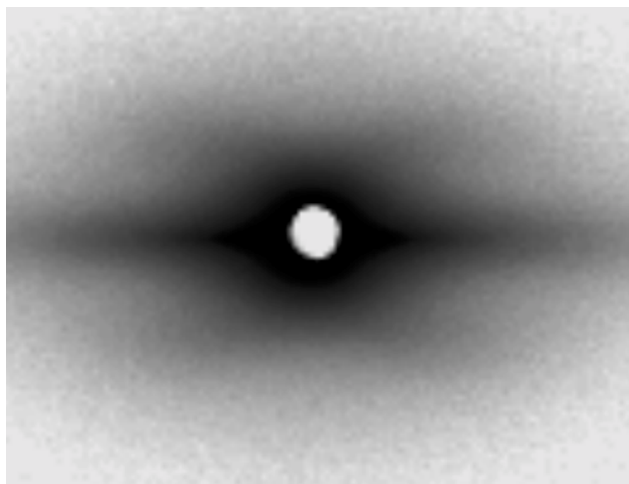
The important points to be discussed now are (1) the morphology of the superstructure generating the four-point pattern and its tilt angle and (2) the nature of its density contrast. Both questions cannot be unambiguously answered based on scattering data alone. Nevertheless, it will be interesting to see which models can be proposed that are compatible with the observed scattering data and any given additional information.

Many possible structures can generate four-point scattering patterns but it turns out that the orientation information of the WAXS patterns and the exact shape of the SAXS four-point pattern allow us to rule out most of them. The present high degree of preferred orientation, assessable from the equatorial WAXS arcs, eliminates any model generating the tilt angle by inclined microfibrils; all molecule chains and, thus, any microfibrils must be highly preferentially oriented about the fiber axis. Possible structures fulfilling these conditions and still producing a four-point scattering pattern are, e.g., the checkerboard and the herringbone pattern. A careful inspection of the SAXS four-point pat-

(a) as-spun



(b) high modulus



(c) extended heat treatment

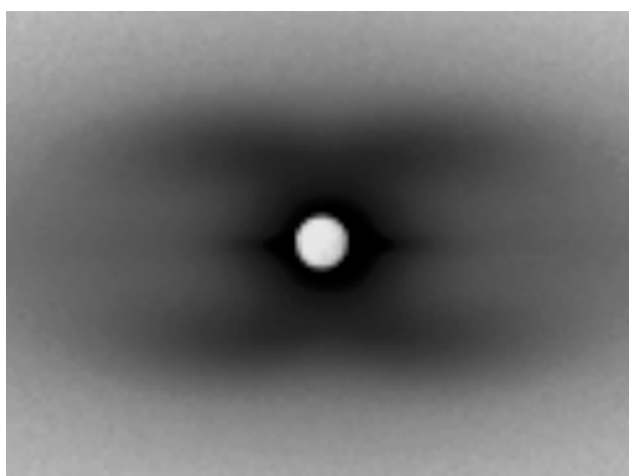
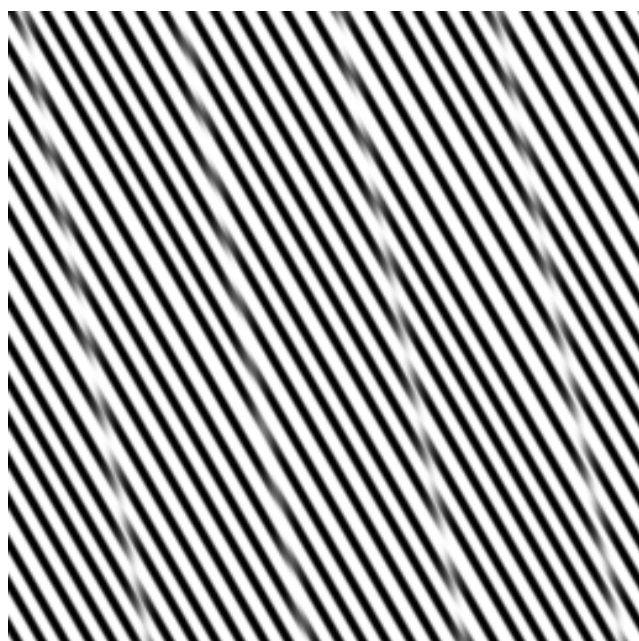


**Figure 5.** SAXS patterns of as-spun (AS), high-modulus (HM), and extended heat treatment (EHT) PBO fibers, the latter two showing a four-point pattern (fiber axis vertical).

terns shows an inclined elongated appearance of the four maxima. This reciprocal space feature can be interpreted in terms of a corresponding inclination of grain boundaries or other boundaries limiting coherent domains in real space. Figure 6(a) shows a simulated density pattern consisting of inclined lamellar stacks (producing the tilt angle) confined by differently inclined grain boundaries (producing the shape of the maxima). Due to these inclined grain boundaries, a herringbone-like alternating arrangement of lamellar inclinations is not practical; neighboring lamellar stacks have to have similar tilt orientations in order to pack densely. Accordingly, the scattering from the pattern in Figure 6(a) only shows a tilted two-point pattern (Figure 6(b)) and the complete four-point pattern is restored after a cylinder

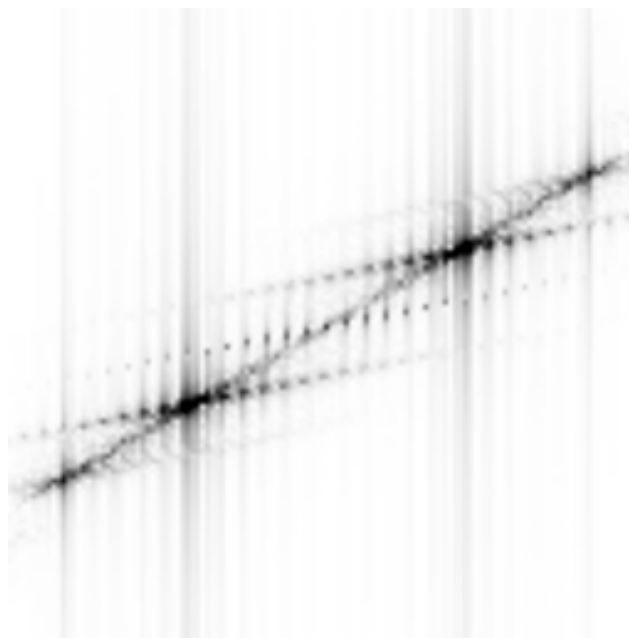
(a) density map



average (Figure 6(c)). It should be noted that these transformations are crude 2D approximations only, valid for a qualitative discussion. A more quantitative description would take into account the cylindrical symmetry, involving Fourier-Bessel transforms, which cannot be performed as Fast Fourier Transforms.

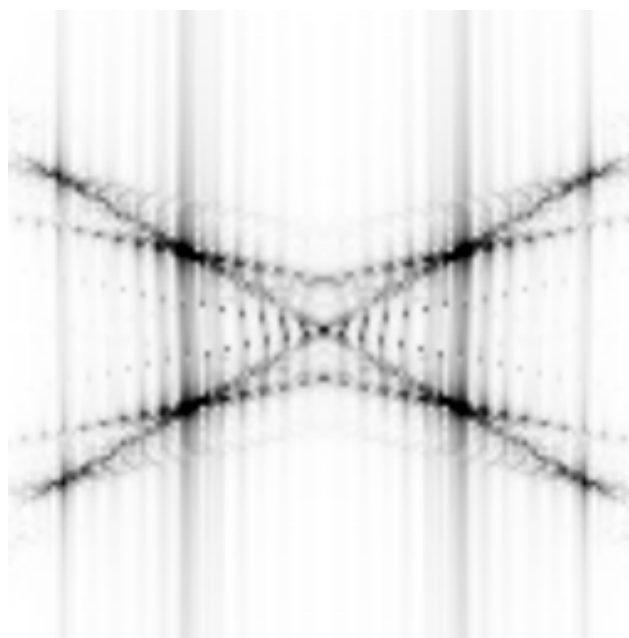
Figure 7 suggests a model, illustrating the complete texture information of a PBO fiber, that is compatible with the experimental SAXS data. It is conceivable that these types of inclinations can be generated by shear forces (due to differing flow velocities as a function of the fiber radius) during the fiber spinning and stretching. A micro-focus SAXS experiment with a primary beam smaller than half the fiber diameter could be useful to verify this model by resolving the four-point pattern into individual two-point patterns. Further work along these lines is in progress.

(b) Two-point pattern



**Figure 6.** (a) A simulated 2D density map with inclined lamellar stacks and inclined grain boundaries. (b) Squared 2D Fourier transform of (a). (c) Mirror or cylindrical average of (b). The various Fourier transformation artifacts in (b) and (c) are expected for this limited model and should not distract from its fundamental features.

(c) Four-point pattern



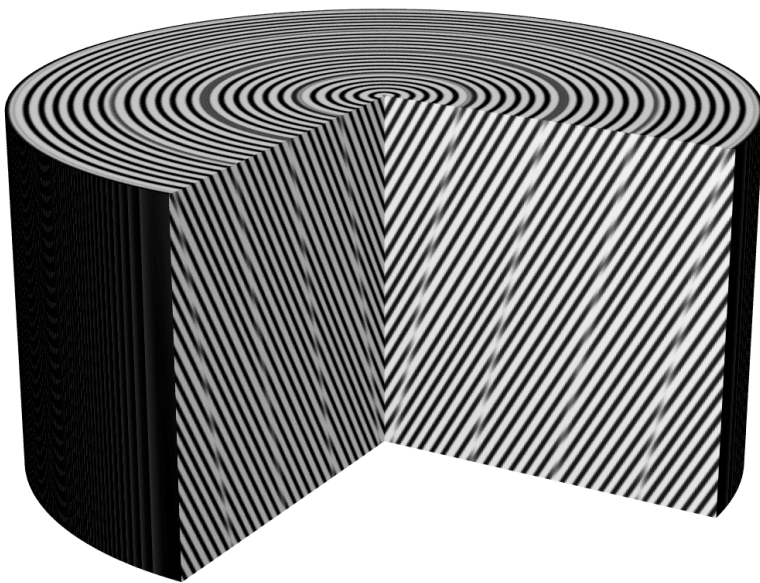


**Figure 7.** Schematic model illustrating the spatial arrangement of the various inclinations present in the density patterns. The flow direction is assumed to be downwards although this information cannot be deduced from a scattering pattern. Note that the PBO molecules are perfectly aligned in the vertical direction; for an explanation of the density contrast see Figure 8.

While the observed tilt angle can be readily and satisfactorily explained by shear deformations, no obvious explanation presents itself for the nature of the density contrast generating the four-point pattern or for the reasons of its formation. It is reasonable to assume that the observed period is the result of a kinetic process reaching the limits of chain ordering due to defects, just like in traditional semi-crystalline polymers. However, due to the lack of conformational degrees of freedom in the PBO molecule itself, excluding any kind of classical chain coiling or entanglement and leaving chain ends as the only significant defects, it must be concluded that the presence of PPA, not hampered by such rigidity constraints, plays an important role in the ordering process, and that the superstructure generating the four-point pattern, which is imprinted by the presence of PPA, persists even after its removal in the coagulation bath.

It is assumed that the crystallization process in the freshly spun uncoagulated fiber produces inclined lamellar stacks where one lamella type consists of an ordered arrangement of well-defined PBO-PPA solvate structures and the other lamella type consists of a less ordered PBO-PPA arrangement with interdispersed coiled and entangled PPA. The removal of PPA results in crystalline PBO lamellae and in slightly less ordered lamellae where the PBO molecules are allowed to assume very gently twisted conformations to accommo-

date slightly different orientations and/or translations between two ordered lamellae. The chain conformation inside the less ordered domains does not significantly reduce the overall preferred orientation. All the chain ends and other possible defects accumulate inside these slightly less ordered lamellae, thereby producing a small density contrast. A schematic representation of this model with the PBO molecules approximated by ribbons is sketched in Figure 8. Note that the model as depicted is also in accordance with a preferred *a*-axis orientation. The contrast enhancement upon heat treatment probably consists mainly of a more complete migration of the chain ends into the less ordered domains and a perfection of the ordered domains, although a beginning chemical reaction cannot be ruled out.

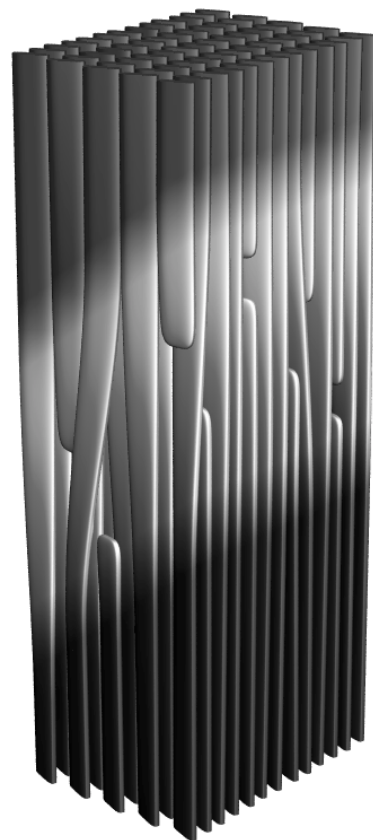


**Figure 8.** Schematic representation of the inclined density contrast between highly ordered regions (dark, top and bottom) and slightly less ordered regions (light) containing chain ends and gently twisted PBO molecules (model is not to scale).

## Conclusions

The models developed in the present study offer a consistent explanation for the structure and its formation in PBO fibers in agreement with experimental scattering data. If the sketches in Figures 7 and 8 turn out to be a good approximation of the reality, it should be clear that the mechanical properties of PBO fibers strongly depend on the exact details of these models. The slight entanglement taking place in the less ordered regions should lead to an improved response of the fiber to shear forces, not causing a graphite-like unrestricted falling apart of the structure but resulting in the shear deformation of coherent parallelogram-shaped regions. This effect, together with the present disorder itself, could also explain how the fiber dissipates energy responding to an impact, a very important property for the designed applications, where a homogeneous crystalline structure would be susceptible to failure due to its brittleness.

## Acknowledgements

Support of this work by the U.S. Army Research Office (DAAD190010419), for the Advanced Polymers Beamline X27C by the U.S. Department of Energy (DOE) (DEFG0299ER45760) and for ChemMat CARS by the National Science Foundation/DOE (CHE9522232, CHE0087817) are gratefully acknowledged. Research carried out in part at the National Synchrotron Light Source, Brookhaven National Laboratory, which is supported by the U.S. Department of Energy, Division of Materials Sciences and Division of Chemical Sciences, under Contract No. DE-AC02-98CH10886.

## Reference

- [1] S. Ran, C. Burger, D. Fang et al., "In-situ Synchrotron WAXD/SAXS Studies of Structural Development during PBO/PPA Solution Spinning" *Macromolecules*, 35(2), 433-439, 2002.